Type-3 Ryanodine Receptors Mediate Hypoxia-, but Not Neurotransmitter-induced Calcium Release and Contraction in Pulmonary Artery Smooth Muscle Cells

Yun-Min Zheng,[1] Qing-Song Wang,[1] Rakesh Rathore,[1] Wan-Hui Zhang,[1] Joseph E. Mazurkiewicz,[1] Vincenzo Sorrentino,[2] Harold A. Singer,[1] Michael I. Kotlikoff,[3] and Yong-Xiao Wang[1]

[1]Center for Cardiovascular Sciences, Neuroscience, and Neuropharmacology, Albany Medical College, Albany, NY 12208
[2]Molecular Medicine Section, Department of Neuroscience, University of Siena, Siena, Italy 53100
[3]Department of Biomedical Sciences, College of Veterinary Medicine, Cornell University, Ithaca, NY 14853

ABSTRACT In this study we examined the expression of RyR subtypes and the role of RyRs in neurotransmitter- and hypoxia-induced Ca^{2+} release and contraction in pulmonary artery smooth muscle cells (PASMCs). Under perforated patch clamp conditions, maximal activation of RyRs with caffeine or inositol triphosphate receptors (IP_3Rs) with noradrenaline induced equivalent increases in $[Ca^{2+}]_i$ and Ca^{2+}-activated Cl^- currents in freshly isolated rat PASMCs. Following maximal IP_3-induced Ca^{2+} release, neither caffeine nor chloro-*m*-cresol induced a response, whereas prior application of caffeine or chloro-*m*-cresol blocked IP_3-induced Ca^{2+} release. In cultured human PASMCs, which lack functional expression of RyRs, caffeine failed to affect ATP-induced increases in $[Ca^{2+}]_i$ in the presence and absence of extracellular Ca^{2+}. The RyR antagonists ruthenium red, ryanodine, tetracaine, and dantrolene greatly inhibited submaximal noradrenaline– and hypoxia-induced Ca^{2+} release and contraction in freshly isolated rat PASMCs, but did not affect ATP-induced Ca^{2+} release in cultured human PASMCs. Real-time quantitative RT-PCR and immunofluorescence staining indicated similar expression of all three RyR subtypes (RyR1, RyR2, and RyR3) in freshly isolated rat PASMCs. In freshly isolated PASMCs from RyR3 knockout ($RyR3^{-/-}$) mice, hypoxia-induced, but not submaximal noradrenaline–induced, Ca^{2+} release and contraction were significantly reduced. Ruthenium red and tetracaine can further inhibit hypoxic increase in $[Ca^{2+}]_i$ in $RyR3^{-/-}$ mouse PASMCs. Collectively, our data suggest that (a) RyRs play an important role in submaximal noradrenaline– and hypoxia-induced Ca^{2+} release and contraction; (b) all three subtype RyRs are expressed; and (c) RyR3 gene knockout significantly inhibits hypoxia-, but not submaximal noradrenaline–induced Ca^{2+} and contractile responses in PASMCs.

KEY WORDS: ryanodine receptor • inositol triphosphate receptor • hypoxia • neurotransmitter • pulmonary artery smooth muscle cell

INTRODUCTION

Ca^{2+} release from the sarcoplasmic/endoplasmic reticulum (SR) through the intracellular Ca^{2+} channels inositol 1,4,5-triphosphate receptors (IP_3Rs) and RyRs is critical for numerous cellular responses. The functional redundancy of these channels substantially complicates the understanding of the physiological role of RyRs in vascular smooth muscle cells (SMCs). We have recently shown that activation of RyRs with caffeine induces Ca^{2+} release and prevents subsequent neurotransmitter-induced responses, and vice versa, in freshly isolated rat pulmonary artery SMCs (Wang et al., 2003), indicating that RyRs and IP_3Rs may be functionally colocalized in the same SR. Similar functional colocalization of both receptors in the same SR has also been found in cultured rat pulmonary artery smooth muscle cells (PASMCs) (Zhang et al., 2003) and other types of vascular myocytes (Leijten and van Breemen, 1984; Amedee et al., 1990; Pacaud and Loirand, 1995; Boittin et al., 1999; Janiak et al., 2001). These findings, together with the fact that Ca^{2+} activates RyRs and induces Ca^{2+} release from the SR, a process termed as Ca^{2+}-induced Ca^{2+} release (CICR), raise a possibility that Ca^{2+} released from IP_3Rs may open the neighboring RyRs and then induce further Ca^{2+} release, contributing to neurotransmitter-induced Ca^{2+} and contractile responses in PASMCs. In support of this hypothesis, a recent study performed in cultured PASMCs has shown that photorelease of caged IP_3 can stimulate RyR-mediated Ca^{2+} sparks (Zhang et al., 2003). However, it should be

Correspondence to Yong-Xiao Wang: wangy@mail.amc.edu

Abbreviations used in this paper: CMC, chloro-*m*-cresol; IP_3R, inositol 1,4,5-triphosphate receptor; PASMC, pulmonary artery smooth muscle cell; PSS, physiological saline solution; RT-PCR, reverse transcriptase PCR; SMC, smooth muscle cell.

J. Gen. Physiol. © The Rockefeller University Press • 0022-1295/2005/04/427/14 $8.00
Volume 125 April 2005 427–440
http://www.jgp.org/cgi/doi/10.1085/jgp.200409232

noted that cell culture may significantly affect expression levels and functions of RyRs in vascular SMCs (Masuo et al., 1991; Cortes et al., 1997; Vallot et al., 2000; Thorne and Paul, 2003).

It is well known that hypoxia exposure induces pulmonary, but not systemic (mesenteric and cerebral) artery vasoconstriction (Madden et al., 1992; Vadula et al., 1993; Yuan et al., 1993; Wang et al., 2003). This unique hypoxia-induced pulmonary vasoconstriction serves as an important physiological process for maintaining arterial oxygenation. We and other investigators have recently shown that the depletion of SR Ca^{2+} with caffeine (through activation of RyRs) reduces or abolishes hypoxia-induced increases in $[Ca^{2+}]_i$ and contraction in PASMCs (Salvaterra and Goldman, 1993; Post et al., 1995; Jabr et al., 1997; Dipp et al., 2001; Wang et al., 2003). Similarly, ryanodine, an agent that binds with high affinity to RyRs, largely or completely inhibits hypoxic responses (Vadula et al., 1993; Jabr et al., 1997; Dipp et al., 2001; Morio and McMurtry, 2002). These data suggest that RyRs possibly play an important role in hypoxic responses in PASMCs.

Three subtypes of RyRs (RyR1, RyR2, and RyR3) are expressed in mammalian cells, each encoded by distinct genes. However, studies on mRNA expression of RyR subtypes in cultured vascular SMCs or vascular tissues have yielded conflicting results, showing expression of RyR1, RyR2, and RyR3 all (Neylon et al., 1995; Coussin et al., 2000; Lohn et al., 2001), abundant RyR3, little RyR2, and no RyR1 (Ledbetter et al., 1994; Vallot et al., 2000), as well as RyR1 only (Vallot et al., 2000). These conflicting data may occur due to the changes in RyR expression patterns and levels during cell culture or due to the contamination with other types of cells in experiments using vascular tissues (Vallot et al., 2000). Nonetheless, little is known about expression patterns and levels of RyR subtypes in PASMCs.

Using the antisense oligonucleotide technique to selectively suppress the expression of RyR subtypes, Coussin et al. (2000) have shown that RyR1 and RyR2, but not RyR3, participate in Ca^{2+} release following activation of voltage-dependent Ca^{2+} currents (I_{Ca}) in cultured portal vein SMCs. However, studies using freshly isolated portal vein and coronary artery myocytes indicate that I_{Ca} fails to induce Ca^{2+} release (Ganitkevich and Isenberg, 1995; Kamishima and McCarron, 1996). It has been reported that caffeine- and noradrenaline-induced arterial muscle contractions are not significantly changed in RyR3 knockout ($RyR3^{-/-}$) mice (Takeshima et al., 1996). In contrast, a recent report has shown that the frequency of Ca^{2+} sparks and STOCs (spontaneous transient outward currents) are increased in $RyR3^{-/-}$ mouse cerebral artery myocytes (Lohn et al., 2001). These discrepancies possibly reflect differential expression patterns and levels of RyR subtypes in systemic artery SMCs, in addition to different experimental conditions. Moreover, physiological functions of RyR subtypes in PASMCs are largely unknown.

In the present study, we first sought to determine physiological functions of RyRs in freshly isolated PASMCs by examining whether these Ca^{2+} release channels were involved in noradrenaline- and hypoxia-induced increases in $[Ca^{2+}]_i$ and contraction using several structurally different RyR blockers. Next we examined mRNA and protein expression patterns and levels of RyR subtypes in freshly isolated PASMCs using real-time quantitative RT-PCR and immunofluorescence staining. Finally, we examined whether RyR3 gene knockout affected noradrenaline- and hypoxia-induced Ca^{2+} and contractile responses in freshly isolated PASMCs. Our data indicate that RyRs may amplify neurotransmitter-induced Ca^{2+} release and contraction in PASMCs, which likely occurs through a local IP_3R–RyR interaction. These Ca^{2+} release channels also play an important role in hypoxia-induced Ca^{2+} release and contraction in PASMCs. All three subtypes of RyRs are expressed in PASMCs, and the amount of mRNA transcript is equivalent. RyR3 gene knockout significantly inhibits hypoxia-, but not noradrenaline-induced Ca^{2+} release and contraction in PASMCs, suggesting a unique function for this RyR subtype.

MATERIALS AND METHODS

Cell Preparation

Freshly isolated cells were obtained from rat resistance (external diameter < 300 μm) pulmonary arteries, since these regional cells show stronger responses to hypoxia (Madden et al., 1985, 1992; Archer et al., 1996). The procedure for cell isolation was similar to that described previously (Wang et al., 2003). Under approved animal care and use protocols, Sprague-Dawley rats were killed by an intraperitoneal injection of sodium pentobarbital (150 mg/kg). Resistance pulmonary arteries were removed and cleaned of the connective tissue and endothelium. Small pieces (1×10 mm) of the arteries were incubated in nominally Ca^{2+}-free physiological saline solution (PSS) containing papain (Sigma-Aldrich) and dithioerythritol at 37°C for 20 min, then in nominally Ca^{2+}-free PSS containing type H and II collagenase (Sigma-Aldrich) and 100 μM Ca^{2+} for 10–15 min (37°C), and finally in ice cold nominally Ca^{2+}-free PSS for 15 min. Single cells were harvested by gentle trituration, and then stored on ice for use up to 8 h. PSS contained (in mM) 125 NaCl, 5 KCl, 1 $MgSO_4$, 10 HEPES, 1.8 $CaCl_2$, and 10 glucose (pH 7.4).

RyR3 knockout ($RyR3^{-/-}$) mice were obtained as described previously (Bertocchini et al., 1997), and maintained as heterozygotes, which were continually backcrossed to generate $RyR3^{-/-}$ and wild-type ($RyR3^{+/+}$) mice. Freshly isolated resistance (third and smaller branches) PASMCs from $RyR3^{-/-}$ and $RyR3^{+/+}$ (same age and sex) mice were prepared using the same procedure as described above.

Cultured human PASMCs were purchased from Cambrex and cultured in smooth muscle growth medium in a humidified atmosphere of 5% CO_2 in air at 37°C. The medium contained 5% FBS, 0.5 ng/ml human epidermal growth factor, 2 ng/ml human

fibroblast growth factor, and 5 μg/ml insulin. Cells at the fifth and sixth passage were used for experiments.

Measurements of Whole-cell $[Ca^{2+}]_i$

Measurements of whole-cell $[Ca^{2+}]_i$ were made by a dual excitation wavelength fluorescence method as described previously (Wang et al., 2003), using the IonOptix fluorescence photometric system (Milton). PASMCs were loaded with 4 μM fura-2/AM for 20 min. The dye was excited at 340- and 380-nm wavelengths (Xenon 75 W arc lamp). The emission fluorescence at 510 nm was detected by a photomultiplier tube. Photo bleaching was minimized by using neutral density filters and by shuttering excitation light between sampling periods. Background fluorescence was determined by removing the cell from the field after the experiment.

Membrane Current Recording

Whole-cell membrane currents were measured using nystatin-perforated or standard patch clamp techniques (Wang et al., 2003) with a patch clamp amplifier (EPC-9; Heka Electronics). For the perforated patch clamp experiments, patch pipettes filled with intracellular solution had a resistance of 2–3 MΩ. Nystatin was included in the pipette solution at a final concentration of 250 μg/ml. When electrical access was detected, cells were clamped at a holding potential of −55 mV. Membrane capacitance and series resistance were continuously monitored and compensated, and experiments initiated following a decrease in the access resistance to <40 MΩ. In some experiments, the standard whole-cell technique was used to dialyze the tested reagents into the cell. In this case, the resistance of the patch pipettes was 1–2 MΩ. The pipette solution contained (in mM) 125 CsCl, 5 NaCl, 1.2 $MgCl_2$, 3 EGTA, 1 $CaCl_2$, and 10 HEPES (pH 7.3) for perforated patch clamp experiments, and 125 CsCl (or KCl), 5 NaCl, 1.2 $MgCl_2$, 3 ATP-Mg, and 10 HEPES (pH 7.3) for standard whole-cell recordings.

Reverse Transcriptase (RT) PCR

The expression of RyR mRNAs in cultured human PASMCs was examined using RT-PCR. Total RNAs were isolated using Absolutely RNA Miniprep Kit (Stratagene). One-step RT-PCR was performed using SuperScript One-Step RT-PCR with Platinum *Taq* (Invitrogen) according to the manufacturer's instructions, supplemented with the following forward and reverse oligonucleotide primers: 5′-GGCTGGTATATGGTGATGTC-3′ and 5′-TCGCTCTTGTTGTAGAACTTGCGG-3′for human RyR1 gene, 5′-ACAGCATGGCCCTTTACAAC-3′ and 5′-TTGGCTTTCTCTTTGGCTGT-3′ for human RyR2 gene, and 5′-CTGTCATCTGTAACTCACAA-3′ and 5′-GTGTCAAAGTAGTCATTGCCAA-3′for human RyR3 gene. The amplified products were electrophoresed on an agarose gel, stained with ethidium bromide, and visualized by UV illumination.

For real-time quantitative RT-PCR experiments, freshly isolated rat resistance PASMCs were used to yield total RNAs to avoid the contamination of neurons, endothelial and other types of cells. Isolated cells were collected using a Burleigh PCS-5300 manipulator under the help of a Nikon inverted microscope. Total RNAs were obtained using Absolutely RNA Nanoprep Kit (Stratagene). The first-strand cDNAs were synthesized from RNAs using SuperScript First-Strand Synthesis System for RT-PCR (Invitrogen). The resultant cDNAs were amplified by specific target gene forward and reverse primers: 5′-TCTTCCCTGCTGGAGACTGT-3′ and 5′-TGGGAGAAGGCACTTGAGG-3′ for rat RyR1 gene, 5′-ACAACCCAAATGCTGGTCTC-3′ and 5′-TCCGGTTCAGACTTGGTTTC-3′ for rat RyR2 gene, and 5′-CTGGCCATCATTCAAGGTCT-3′ and 5′-GTCTCCATGTCTTCCCGTA-3′ for rat RyR3 gene, with the iQ SYBR Green Supermix (Bio-Rad Laboratories, Inc.) using an iCycler iQ Real-time PCR Detection System (Bio-Rad Laboratories, Inc.). The housekeeping gene glyceraldehyde-3-phosphate dehydrogenase (GAPDH) was used as endogenous control. To quantify the target gene mRNA levels, known RyR1, RyR2, RyR3, and GADPH DNAs were used for constructing standard curves. Known DNAs and unknown sample cDNAs at series dilutions (1:10) were simultaneously amplified. Real-time PCR was run for one cycle at 95°C for 3 min followed immediately by 40 cycles at 95°C for 20 s, 58°C (to be varied with different primers) for 20 s, and 72°C for 20 s. The fluorescence was measured after each of the repetitive cycles. A melting point dissociation curve generated by the instrument was used to confirm that only a single product was present. To validate the specificity, no reverse transcriptase and no template control experiments were performed to confirm no fluorescence resulting from either genomic DNA contamination or PCR step. The PCR amplification products were also verified by electrophoresis and sequencing analysis. The absolute expression levels of subtype RyR mRNAs in cells were calculated from standard curves of known DNAs. The absolute mRNA expression levels of target genes were also normalized to levels of GADPH mRNAs to yield the relative levels of target genes.

Immunofluorescence Staining

The experimental protocol was similar to that described previously (Zhang et al., 2001). In brief, freshly isolated rat PASMCs were fixed in 4% paraformaldehyde in PSS for 15 min at room temperature, incubated with 0.2% Triton X-100 in PSS for 30 min, and then blocked for 1 h with 2.5% BSA PSS. After that, cells were incubated with specific primary antibody at 4°C overnight, followed by Alexa488- or Alexa594-conjugated anti-mouse or anti-rabbit antibody (1:750 dilution) (according to the host species of primary antibody) for 2 h. Immunofluorescence staining was examined using Zeiss LSM510 laser scanning confocal microscope. The z interval was adjusted to 1 μm to obtain sufficient fluorescence signals. Alexa488 and Alexa594 were excited at 488 and 543 nm using a krypton-argon laser, and fluorescence was detected using 505 and 585-nm bandpass filters, respectively.

Smooth Muscle Tension Measurements

The third branches of rat or mouse pulmonary arteries were sectioned into segments 3 mm in length, and placed in 2-ml tissue baths (Radnoti). One end of the muscle strip was fixed to a small clip, and the other end connected to a highly sensitive force transducer (Harvard Apparatus). The bath solution contained (in mM): 110 NaCl, 3.4 KCl, 2.4 $CaCl_2$, 0.8 $MgSO_4$, 25.8 $NaHCO_3$, 1.2 KH_2PO_4, and 5.6 glucose (pH 7.4), aerated with 20% O_2, 5% CO_2, and 75%N_2, and warmed at 35°C. The strips were set at a resting tone of 250 mg. Contractile force was recorded using a PowerLab/4SP recording system (AD Instruments). In experiments examining noradrenaline-induced muscle contraction, concentration–response curves were constructed by fitting the mean values of data with Origin Version 7 software (OriginLab Corporation), using the nonlinear Boltzmann equation: $y = A2 + (A1 - A2)/(1 + \exp((x - x_{50})/dx))$, where A1 was minimal noradrenaline-induced contraction, A2 maximal contraction, x the logarithm of noradrenaline concentration, x_{50} the logarithm of concentration for half-maximal contraction (EC_{50}), and dx the slope factor of the curve.

Hypoxia

In experiments using freshly isolated PASMCs, hypoxia was achieved by switching a perfusing solution from a bath solution

equilibrated with 20% O_2, 5% CO_2, and balance with N_2 (normoxic) to a solution equilibrated with 1% O_2, 5% CO_2, and balance with N_2 mixtures (hypoxic). For muscle strip experiments, hypoxia was achieved by switching the bath solution gas mixtures from 20% O_2, 5% CO_2, and 75% N_2 to 1% O_2, 5% CO_2, and 94% N_2. The oxygen tension of the solution was continuously monitored by means of an oxygen electrode (OXEL-1, WPI). The bath Po_2 was ≥140 and 10–20 Torr in the normoxic and hypoxic solution, respectively (Wang et al., 2000).

Reagents and Antibodies

Alexa488- and Alexa594-conjugated anti-mouse and anti-rabbit antibodies, as well as fura-2/AM were obtained from Molecular Probes; IP_3 and ruthenium red from Calbiochem; anti-RyR1 antibody from Upstate Biotechnology; anti-actin (smooth muscle) antibody, anti-myosin (smooth) antibody, caffeine, chloro-*m*-cresol, dantrolene, noradrenaline, nystatin, ryanodine, and tetracaine from Sigma-Aldrich. Anti-RyR2 and anti-RyR3 antibodies were provided by A.F. Lai (University of Wales, Cardiff, UK). The isoform-specific RyR antibodies were tested for confirmation of their specificity.

Data Analysis

All values were expressed as means ± SEM of *n* samples investigated. Student's *t* test was used to determine the significance of differences between two observations, whereas one-way ANOVA was used for multiple comparisons. A P value of <0.05 was considered to be significant.

RESULTS

Ryanodine Receptors and Inositol Triphosphate Receptors Functionally Overlap in PASMCs

Previous studies have shown that activation of RyRs with caffeine, similar to activation of IP_3Rs with noradrenaline, induces Ca^{2+} release from the SR in freshly isolated canine and rat PASMCs (Janiak et al., 2001; Wang et al., 2003). Here we sought to compare the extent of Ca^{2+} release following maximal activation of RyRs and IP_3Rs. Freshly isolated rat PASMCs were loaded with fura-2/AM and voltage clamped at −55 mV using the perforated patch clamp technique. Cs^+ patch pipette solution was used to block outward K^+ currents. Under these conditions, application of caffeine (10 mM) induced an increase in $[Ca^{2+}]_i$ and an inward Ca^{2+}-activated Cl^- current ($I_{Cl(Ca)}$) (Wang et al., 1997b, 2003). A typical example of these experiments is shown in Fig. 1 A. In a total of 16 cells tested, the mean increase in $[Ca^{2+}]_i$ was 702 ± 27 nM (from a resting level of 112 ± 17 to 815 ± 29 nM), and the current had a mean amplitude of 581 ± 42 pA (Fig. 1 B). Stimulation of adrenergic receptors with noradrenaline (300 μM) to activate IP_3Rs induced Ca^{2+} and current responses with similar amplitudes to caffeine-induced responses (Fig. 1 A). The mean increase in $[Ca^{2+}]_i$ following application of noradrenaline was 674 ± 43 nM, and mean amplitude of $I_{Cl(Ca)}$ was 613 ± 33 pA (n = 17) (Fig. 1 B). Thus, maximal activation of RyRs with caffeine and IP_3Rs with noradrenaline induces equivalent Ca^{2+} release and associated $I_{Cl(Ca)}$, which is consistent with previous findings (Janiak et al., 2001; Wang et al., 2003) and suggests that RyRs are highly expressed in PASMCs.

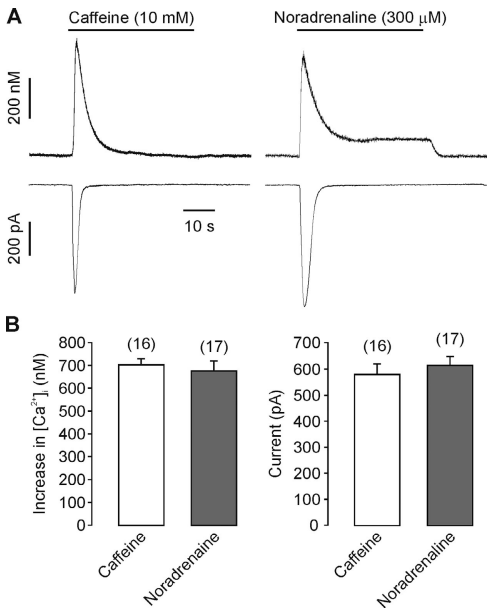

FIGURE 1. Activation of ryanodine receptors with caffeine and inositol triphosphate receptors with noradrenaline induce equivalent increases in $[Ca^{2+}]_i$ and Ca^{2+}-activated Cl^- currents in freshly isolated rat pulmonary artery smooth muscle cells. (A) Original recordings show caffeine- and noradrenaline-induced increases in $[Ca^{2+}]_i$ and $I_{Cl(Ca)}$. Both cells were loaded with fura-2/AM and voltage clamped at −55 mV using the perforated patch clamp technique. Cs^+ pipette solution was used to block K^+ currents. (B) Summary of caffeine- and noradrenaline-induced Ca^{2+} and current responses. Numbers in parentheses indicate the number of cells tested.

Our recent study has shown that prior application of noradrenaline blocks subsequent caffeine-induced Ca^{2+} release in freshly isolated rat PASMCs, and vice versa, indicating that both RyRs and IP_3Rs may functionally overlap (Wang et al., 2003). To further test this view, we examined the effect of IP_3 on caffeine-induced Ca^{2+} release in freshly isolated rat PASMCs. In these experiments, voltage-clamped (−55 mV) myocytes were first dialyzed with IP_3 to induce Ca^{2+} release through IP_3Rs selectively, and then exposed to caffeine. As shown in Fig. 2 A, dialysis of IP_3 induced a Ca^{2+}-activated Cl^- current (Ca^{2+} release). The mean amplitude of the currents was 507 ± 52 pA (n = 5). However, subsequent application of caffeine failed to induce any response in all five cells tested. In converse experiments, cells were first exposed to caffeine and then dialyzed with IP_3. Caffeine-induced Ca^{2+} release was assessed by examining the activity of single Ca^{2+}-activated K^+ (K_{Ca}) channels under cell-attached patch clamp conditions, using K^+ patch pipette solution. Application of caffeine (10 mM) caused a burst increase in activity of single K_{Ca} channels in a cell (Fig. 2 B). The mean current ampli-

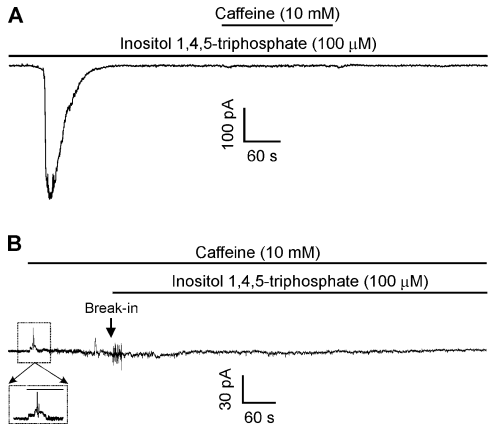

FIGURE 2. Ryanodine receptors and inositol triphosphate receptors are functionally colocalized in freshly isolated rat pulmonary artery myocytes. (A) In a voltage-clamped (−55 mV) cell, dialysis of inositol triphosphate (100 μM) evoked a Ca^{2+}-activated Cl^- current (Ca^{2+} release). However, subsequent application of caffeine (10 mM) failed to induce any further response. (B) On the cell-attached configuration, application of caffeine (10 mM) induced a burst increase in the activity of Ca^{2+}-activated K^+ channels in a cell (holding potential: −20 mV), indicating Ca^{2+} release. In the continued presence of caffeine, however, dialysis of inositol triphosphate (100 μM) following membrane rupture was unable to induce any response (holding potential: −55 mV). K^+ intracellular solution was used in these experiments.

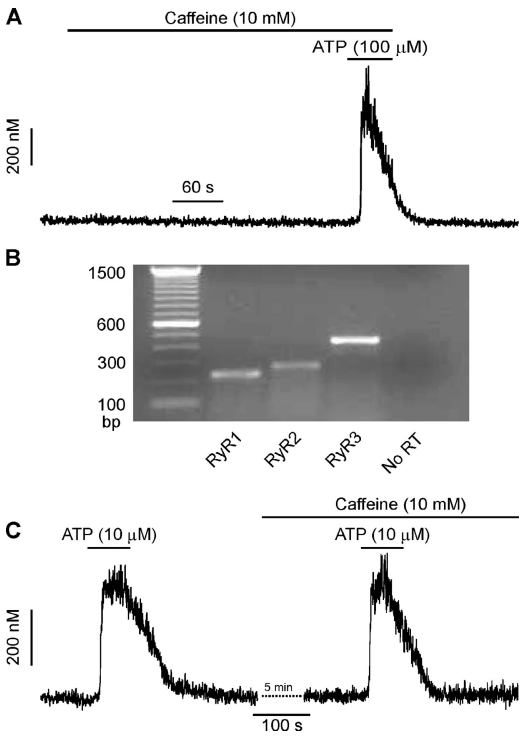

FIGURE 3. Caffeine does not inhibit ATP-induced increases in $[Ca^{2+}]_i$ in cultured human pulmonary artery myocytes that lack functional expression of ryanodine receptors. (A) Original recording shows that application of caffeine (10 mM) could not induce an increase in $[Ca^{2+}]_i$ in a cultured human PASMC. In the same cell, however, application of ATP (100 μM) evoked a large response in the continued presence of caffeine. (B) RyR1, RyR2, and RyR3 mRNAs are detected in cultured human PASMCs by RT-PCR. Total RNAs were amplified with oligonucleotide primers for human RyR1, RyR2, and RyR3 mRNAs, as described in MATERIALS AND METHODS. The PCR products were separated by gel electrophoresis, stained with ethidium bromide, and visualized by UV illumination. Predicted sizes of RyR1, RyR2, and RyR3 were 224, 265, and 431 bp, respectively. No product was found if reverse transcriptase was omitted (No RT). (C) ATP (10 μM) induced increases in $[Ca^{2+}]_i$ in a cell before and after treatment with caffeine (10 mM).

tude in a total of five cells was 23 ± 4 pA. Following the caffeine response, the cell membrane was ruptured to obtain the whole-cell patch clamp configuration, and IP_3 (100 μM) was dialyzed into the cell through the patch pipette. However, dialysis of IP_3 failed to induce any current in the continued presence of caffeine. These results are consistent with our previous findings (Wang et al., 2003), further indicating that both RyRs and IP_3Rs functionally overlap in rat PASMCs.

It has been reported that caffeine may inhibit IP_3-induced Ca^{2+}-activated Cl^- currents (Ca^{2+} release) in *Xenopus* oocytes (Parker and Ivorra, 1991), cerebellum IP_3Rs reconstituted in planar lipid bilayers (Bezprozvanny et al., 1994), and IP_3-induced Ca^{2+} release in permeabilized A7r5 cells in the absence of ATP (Missiaen et al., 1994). To exclude the possibility that IP_3 activity was blocked by caffeine, we examined the effect of chloro-*m*-cresol (CMC), another RyR activator without reported actions on IP_3Rs, on noradrenaline-induced increase in $[Ca^{2+}]_i$. Application of CMC (1 mM) induced an increase in $[Ca^{2+}]_i$ in freshly isolated rat PASMCs. The mean increase in $[Ca^{2+}]_i$ by CMC was 755 ± 67 nM (n = 6). In the continued presence of CMC, however, application of noradrenaline (300 μM) no longer evoked Ca^{2+} release in six cells tested. On the other hand, application of noradrenaline induced an increase in $[Ca^{2+}]_i$ with a mean amplitude of 686 ± 70 nM, and prevented subsequent CMC-induced responses in seven cells tested.

It is known that cell culture may result in significant changes in RyR expression levels and patterns in vascular SMCs, as caffeine fails to induce Ca^{2+} release (Masuo et al., 1991; Cortes et al., 1997; Vallot et al., 2000). Thus, we sought to utilize the cultured human PASMCs as an alternative approach to examine if caffeine could inhibit neurotransmitter-induced Ca^{2+} release. Application of caffeine (10 mM) could not evoke an increase in $[Ca^{2+}]_i$ in a cultured human PASMC, although subsequent application of ATP (100 μM) induced a large response in the same cell (Fig. 3 A). Similar observations were obtained from six other cells. Moreover, CMC (1 mM) was also unable to induce any Ca^{2+} release (n = 6). We then examined the expression of RyRs in cultured human PASMCs using RT-PCR. As shown in Fig. 3 B, the PCR products for RyR1, RyR2, and RyR3 genes

with the predicted sizes of 224, 265, and 431 bp were found. These data indicate that cultured human PASMCs lack responses to RyR agonists, although they express RyR mRNAs, which are consistent with previous reports in cultured rat aortic SMCs (Masuo et al., 1991; Cortes et al., 1997; Vallot et al., 2000).

Using these cultured human myocytes, we examined the effect of caffeine on neurotransmitter-induced Ca^{2+} release. As an example shown in Fig. 3 C, application of ATP (10 μM) induced similar increases in $[Ca^{2+}]_i$ in a cell before and after exposure of caffeine (10 mM) for 5 min. The mean increases in $[Ca^{2+}]_i$ before and after treatment of caffeine were 378 ± 29 and 398 ± 13 nM, respectively ($P > 0.05$, $n = 5$). Similarly, ATP-induced increase in $[Ca^{2+}]_i$ in the absence of extracellular Ca^{2+} (nominally Ca^{2+}-free bath solution containing 1 mM EGTA) to prevent Ca^{2+} influx was not affected by treatment with caffeine (10 mM) for 5 min (unpublished data). These results suggest that caffeine has no inhibitory effect on ATP-mediated Ca^{2+} release through IP_3Rs. Taken together, we believe that the failure of noradrenaline or IP_3 to induce an effect in the presence of caffeine is not due to the direct inhibition of IP_3-mediated Ca^{2+} release. Rather, these data further support the view that prior application of caffeine to activate RyRs may deplete SR Ca^{2+}, and then block subsequent IP_3-induced Ca^{2+} release. Thus, RyR- and IP_3-sensitive Ca^{2+} stores appear to overlap functionally in rat PASMCs.

Ryanodine Receptors Amplify Submaximal Neurotransmitter–induced Ca^{2+} Release and Contraction in PASMCs

The functional colocalization of RyRs and IP_3Rs in the SR, together with the known function of RyRs in mediating Ca^{2+}-induced Ca^{2+} release in SMCs (Imaizumi et al., 1998; Collier et al., 2000), led us to hypothesize that Ca^{2+} released from IP_3Rs during stimulation of neurotransmitter receptors might activate neighboring RyRs, contributing to neurotransmitter-induced responses. To test this hypothesis, we first examined the effect of the RyR antagonist ruthenium red on noradrenaline-induced increase in $[Ca^{2+}]_i$ in freshly isolated rat PASMCs. As shown in Fig. 4 A, repeated application of noradrenaline (10 μM) induced consistent increases in $[Ca^{2+}]_i$ in a control cell. Similar observations were obtained from eight other cells (Fig. 4 C). In contrast, noradrenaline induced a smaller increase in $[Ca^{2+}]_i$ in a cell after treatment with ruthenium red (50 μM) for 5 min (Fig. 4 B). The average increases in $[Ca^{2+}]_i$ following noradrenaline (10 μM) exposure were 436 ± 44 nM before ruthenium red treatment and 141 ± 17 nM after ruthenium red treatment ($P < 0.05$, $n = 10$) (Fig. 4 C). Similarly, pretreatment with the structurally different RyR antagonists ryanodine (100 μM) and tetracaine (10 μM) also significantly inhibited submaximal noradrenaline (10 μM)–induced increases in $[Ca^{2+}]_i$ (Fig. 4 C).

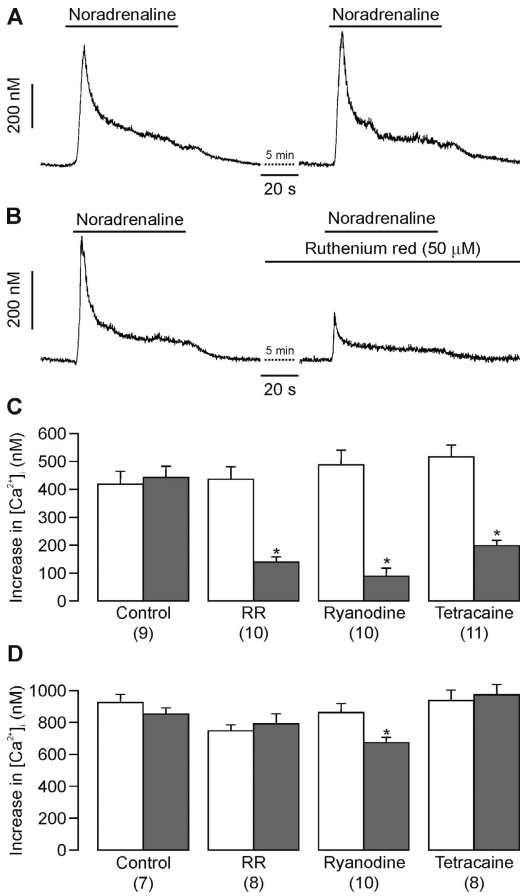

FIGURE 4. Ryanodine receptor antagonists inhibit submaximal noradrenaline–induced increases $[Ca^{2+}]_i$ in freshly isolated rat pulmonary artery smooth muscle cells. (A) Recording trace shows that repeated application of noradrenaline (10 μM) induced consistent increases in $[Ca^{2+}]_i$. Both responses had similar amplitudes. (B) Noradrenaline (10 μM) induced increases in $[Ca^{2+}]_i$ in a cell before and after treatment with ruthenium red (50 mM) for 5 min. Note that noradrenaline response was smaller after treatment of ruthenium red. (C) Summary of the effects of ruthenium red (RR, 50 μM), ryanodine (100 μM), and tetracaine (10 μM) on submaximal noradrenaline (10 μM)–induced increases in $[Ca^{2+}]_i$. *, $P < 0.05$ compared with before treatment with RyR antagonists (open bar). (D) Graph summarizes the effects of RyR antagonists on maximal noradrenaline (300 μM)–induced increases in $[Ca^{2+}]_i$.

However, ruthenium red and tetracaine, unlike ryanodine, did not significantly affect maximal noradrenaline (300 μM)–induced Ca^{2+} release (Fig. 4 D). Thus, RyRs may amplify Ca^{2+} release following submaximal stimulation of adrenergic receptors with noradrenaline in PASMCs, which occurs through the local IP_3R–RyR interaction (Ca^{2+}-induced Ca^{2+} release mechanism).

We next examined the effects of RyR antagonists on noradrenaline-induced muscle contraction in rat pulmonary artery strips. As shown in Fig. 5, in the presence of ruthenium red (50 μM), ryanodine (100 μM), tetracaine (10 μM), or dantrolene (10 μM) for 10 min

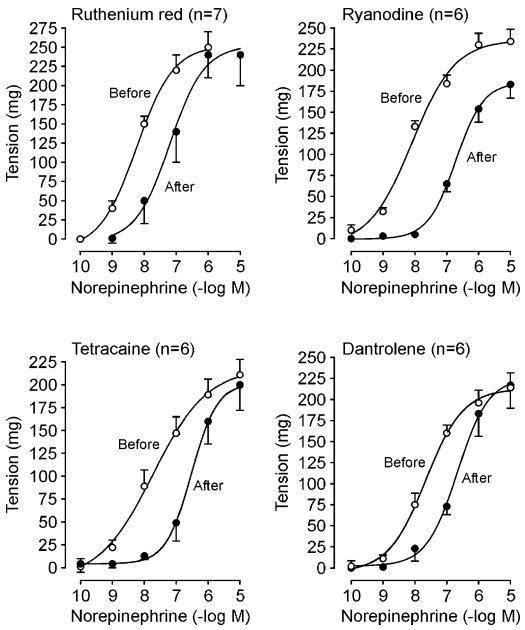

FIGURE 5. Ryanodine receptor antagonists inhibit noradrenaline-induced muscle contraction in freshly isolated rat pulmonary artery strips. Concentration–response curves for noradrenaline-induced muscle contraction were obtained before and after treatment of ruthenium red (50 μM), ryanodine (100 μM), tetracaine (10 μM), or dantrolene (10 μM) for 10 min. Data points represent the mean values of six or seven identical experiments. The continuous lines were curves fitted to a nonlinear Boltzmann equation (see MATERIALS AND METHODS).

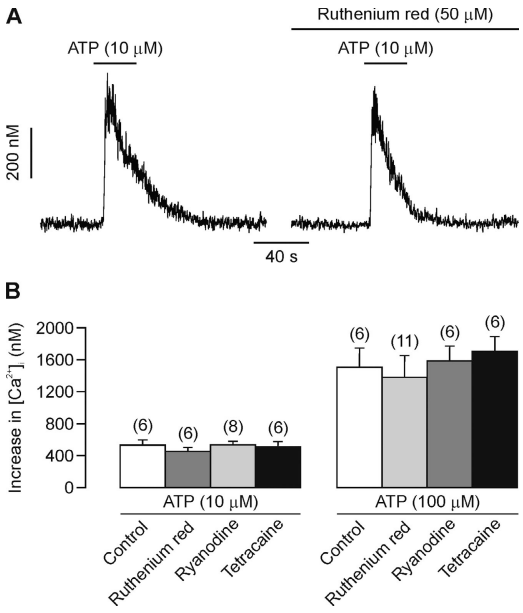

FIGURE 6. Ryanodine receptor antagonists do not inhibit ATP-induced increases in $[Ca^{2+}]_i$ in cultured human pulmonary artery smooth muscle cells. (A) Original recording shows that ATP (10 μM) induced increases in $[Ca^{2+}]_i$ in a control cell and a cell pretreated with ruthenium red (50 μM) for 5 min. (B) Summary of the effects of ruthenium red (50 μM), ryanodine (100 μM), and tetracaine (10 μM) on ATP (10 and 100 μM)-induced increases in $[Ca^{2+}]_i$.

to block RyRs, concentration–response curves for noradrenaline-induced muscle contraction were shifted to the right. Ruthenium red, tetracaine, and dantrolene did not affect noradrenaline-induced maximal responses, while ryanodine reduced the maximum contraction. These data further suggest that Ca^{2+} release following submaximal stimulation of neurotransmitter receptors is able to open the neighboring RyRs, which causes further Ca^{2+} release from the SR and then amplifies neurotransmitter-induced increase in $[Ca^{2+}]_i$ and associated contraction in PASMCs.

Since RyR antagonists have been reported to inhibit IP_3Rs directly or indirectly (Vites and Pappano, 1992; Yamazawa et al., 1992; Iino et al., 1994; Tovey et al., 2000; Zimmermann, 2000; Flynn et al., 2001), we sought to examine the specificity of the RyR antagonists on neurotransmitter-induced Ca^{2+} release in cultured human PASMCs, since these cells lack functional expression of RyRs (Fig. 3). Application of ATP induced similar increases in $[Ca^{2+}]_i$ in a control cell and a cell pretreated with ruthenium red (50 μM) for 5 min (Fig. 6 A). The mean increases in $[Ca^{2+}]_i$ by ATP (10 μM) were 522 ± 72 in six control cells and 452 ± 48 nM in six cells pretreated with ruthenium red, respectively ($P > 0.05$). Similarly, ATP (100 μM)-induced increases in $[Ca^{2+}]_i$ were not affected by ruthenium red (50 μM) (Fig. 6 B). Moreover, treatment with ryanodine (100 μM) and tetracaine (10 μM) for 5 min had no effect on ATP-induced increases in $[Ca^{2+}]_i$ (Fig. 6 B). These results indicate that the RyR antagonists block neurotransmitter-induced Ca^{2+} release and contraction in PASMCs by specifically inhibiting RyRs, rather than by affecting IP_3Rs.

Ryanodine Receptors Mediate Hypoxia-induced Ca^{2+} Release and Contraction in PASMCs

It has been reported that pretreatment with caffeine and ryanodine can inhibit hypoxic increase in $[Ca^{2+}]_i$ in PASMCs (Salvaterra and Goldman, 1993; Vadula et al., 1993; Cornfield et al., 1994; Wang et al., 2003) and hypoxic vasoconstriction in isolated pulmonary artery strips and lungs (Jabr et al., 1997; Dipp et al., 2001; Morio and McMurtry, 2002). Considering that the inhibitory effects of these compounds could occur due to the depletion of SR Ca^{2+}, we sought to use ruthenium red and tetracaine, the RyR antagonists that do not open the channels and deplete SR Ca^{2+}, to examine hypoxic increase in $[Ca^{2+}]_i$ in freshly isolated rat PASMCs. Fig. 7 A shows examples of hypoxia-induced increase in $[Ca^{2+}]_i$ in a control cell and a cell pretreated with ruthenium red (50 μM) for 5 min. Ruthenium red significantly inhibited hypoxia-induced response. As summarized in Fig. 7 B, hypoxia-induced increases in $[Ca^{2+}]_i$ were 442 ± 19 nM in control cells and 188 ± 12 nM in

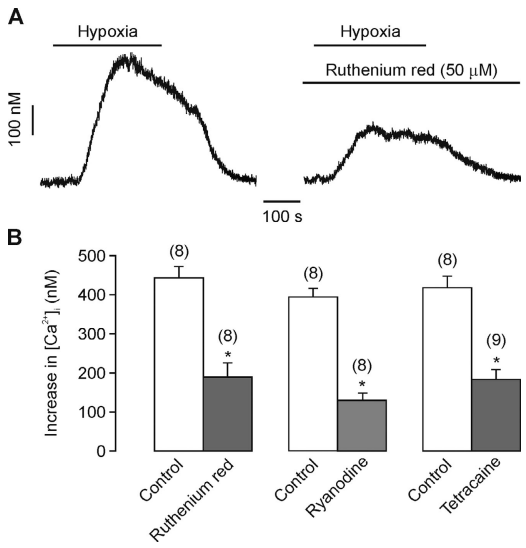

FIGURE 7. Ryanodine receptor antagonists inhibit hypoxic increases in $[Ca^{2+}]_i$ in freshly isolated rat pulmonary artery smooth muscle cells. (A) Original recordings show hypoxia-induced increases in $[Ca^{2+}]_i$ in a control cell and a cell pretreated with ruthenium red (50 μM) for 5 min. (B) Summary of the effects of ruthenium red (50 μM), ryanodine (100 μM), and tetracaine (10 μM) on hypoxic responses. *, $P < 0.05$ compared with control (open bar).

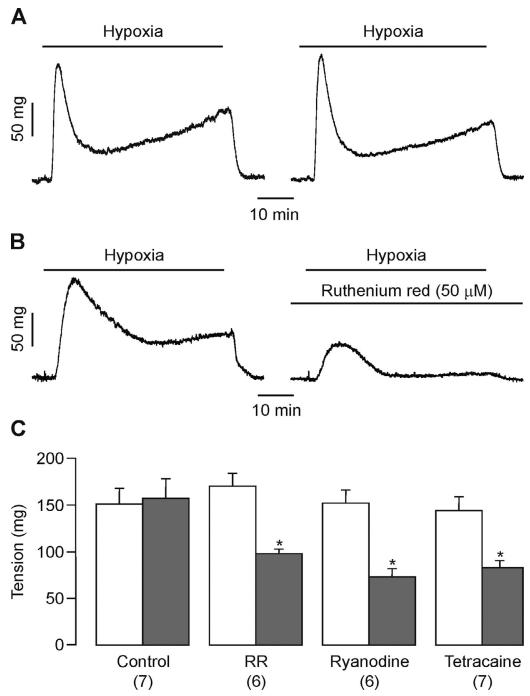

FIGURE 8. Ryanodine receptor antagonists inhibit hypoxic vasoconstriction in freshly isolated rat pulmonary artery strips. (A) Original recordings show that repeated hypoxia induced vasoconstrictions with similar amplitudes in a pulmonary artery strip. (B) Hypoxic vasoconstrictions were recorded in a pulmonary artery strip before and after treatment with ruthenium red (50 μM) for 10 min. (C) Summary of the effects of ruthenium red (50 μM), ryanodine (100 μM), and tetracaine (10 μM) on hypoxic pulmonary vasoconstrictions. *, $P < 0.05$ compared with before treatment with RyR antagonists (open bar).

ruthenium red–treated cells ($n = 8$, $P < 0.05$). Similarly, pretreatment with ryanodine (100 μM) and tetracaine (10 μM) for 5 min to block RyRs also inhibited hypoxia-induced increases in $[Ca^{2+}]_i$ (Fig. 7 B). Therefore, hypoxia may result in the opening of RyRs and subsequent Ca^{2+} release in PASMCs.

In the next experiments, we investigated the effect of RyR antagonists on hypoxic vasoconstriction in freshly isolated rat pulmonary artery strips. In control muscle strips, repeated hypoxic exposure induced consistent vasoconstrictions (Fig. 8). However, in muscle strips pretreated with ruthenium red (50 μM) for 10 min, hypoxic pulmonary vasoconstriction was markedly inhibited. In a total of seven identical experiments, hypoxic vasoconstrictions were decreased from 170 ± 14 mg before treatment with ruthenium red to 98 ± 5 mg after treatment with ruthenium red ($P < 0.05$) (Fig. 8 C). Similarly, ryanodine (100 μM) and tetracaine (10 μM) also significantly blocked hypoxic vasoconstrictions. Taken together, these data suggest that RyRs serve as an important target for hypoxia, by which these Ca^{2+} release channels are opened during hypoxic stimulation, contributing to hypoxic increase in $[Ca^{2+}]_i$ and contraction in PASMCs.

All Three Subtypes of Ryanodine Receptors Are Expressed in PASMCs

To further determine expression patterns and levels of RyR subtype expression in PASMCs, we examined the expression of RyR1, RyR2, and RyR3 mRNAs in freshly isolated rat myocytes using real-time quantitative RT-PCR. Freshly isolated cells were used to avoid potential contaminations with neuronal, endothelial, and other types of cells as well as to avoid significant changes in expression patterns and levels of RyRs during cell culture. To verify that the elongated cells freshly isolated from pulmonary arteries were SMCs, we examined the expression of smooth muscle actin and myosin in these cells using immunofluorescence staining. As expected, both smooth muscle–specific markers were expressed in these cells (Fig. 9 A). Using these cells (PASMCs) as a source of mRNAs, RyR1, RyR2, and RyR3 were amplified by PCR, indicating the presence of all three RyR subtype mRNAs in PASMCs. In addition, absolute mRNA expression levels of RyR subtypes, which were calculated from standard curves of known DNAs, were similar. Similarly, there were no differences between relative mRNA expression levels of all three RyR subtypes, which were generated by normalizing their mRNA levels to GADPH mRNA levels ($n = 8$, Fig. 9 B). The amplification products of RyR subtypes were further examined by gel electrophoresis. Predicted sizes of

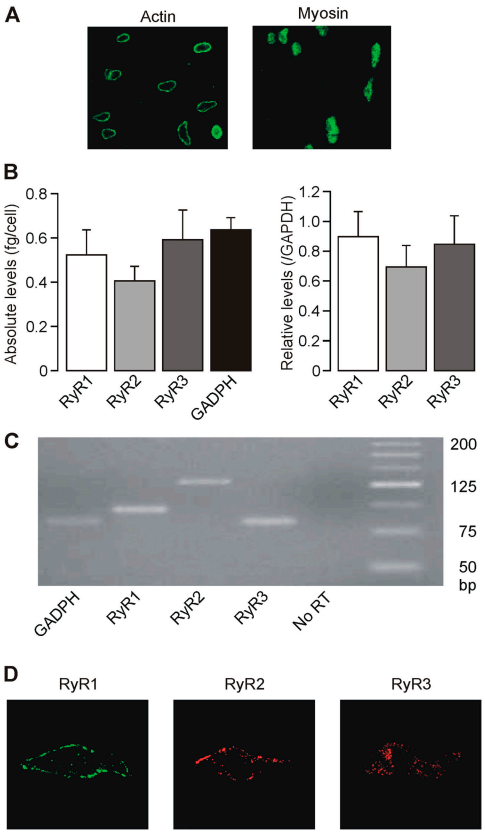

FIGURE 9. All three subtypes of ryanodine receptors are expressed in freshly isolated rat pulmonary artery smooth muscle cells. (A) Expression of smooth muscle–specific actin and myosin in freshly isolated cells from pulmonary arteries was examined by using immunofluorescence staining. Both smooth muscle–specific markers were present in these cells, further conforming that these cells were PASMCs. (B) RyR1, RyR2, and RyR3 mRNA expression was examined by using real-time quantitative RT-PCR. Total RNAs were obtained from freshly isolated rat PASMCs. Absolute mRNA levels of RyR subtypes (left) were calculated from standard curves of known DNAs. Relative mRNA levels (right) were generated by normalizing RyR subtype mRNA levels to GADPH mRNA levels (n = 8). (C) The RyR1, RyR2, and RyR3 PCR products were verified by gel electrophoresis. Predicted sizes of GAPDH, RyR1, RyR2, and RyR3 were 87, 93, 130, and 83 bp, respectively. No product was detected if reverse transcriptase was omitted (No RT). (D) Examination of RyR1, RyR2, and RyR3 protein expression using immunofluorescence staining. RyR subtypes were probed with specific anti-RyR1, anti-RyR2, and anti-RyR3 antibodies. Images were taken using a Carl Zeiss MicroImaging, Inc. LSM510 confocal microscope.

the RyR1, RyR2, and RyR3 PCR products were 93, 130, and 83 bp, respectively (Fig. 9 C). Moreover, sequencing analysis confirmed that the PCR products matched the known RyR1, RyR2, and RyR3 mRNA sequences. To complement mRNA expression patterns of RyR subtypes, we studied the expression of RyR1, RyR2, and RyR3 proteins in freshly isolated PASMCs using immunofluorescence staining. As examples show in Fig. 9 D, all RyR1, RyR2, and RyR3 proteins were detected. Similar observations were made in three or four separate

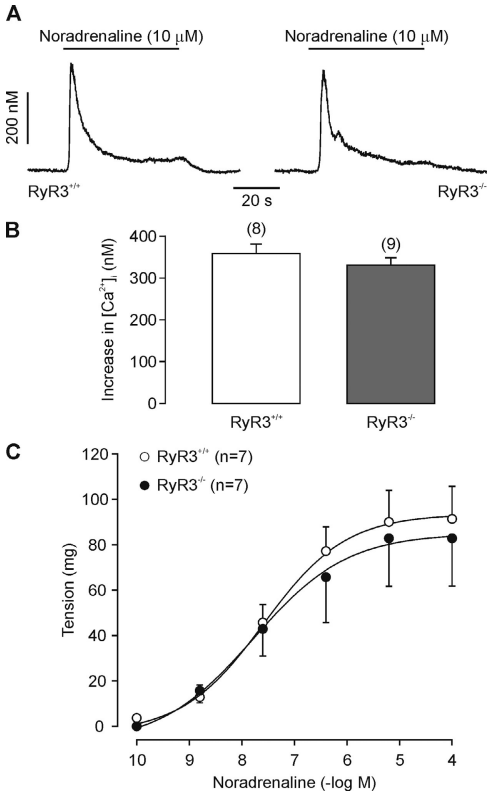

FIGURE 10. Type-3 ryanodine receptor gene knockout does not affect submaximal noradrenaline–induced Ca^{2+} release and contraction in freshly isolated mouse pulmonary artery myocytes. (A) Original recordings show noradrenaline (10 μM)-induced increases in $[Ca^{2+}]_i$ in a pulmonary artery myocyte from wild-type ($RyR3^{+/+}$) and $RyR3^{-/-}$ mouse. (B) Summary of noradrenaline (10 μM)-induced Ca^{2+} responses in PASMCs from $RyR3^{+/+}$ and $RyR3^{-/-}$ mice. (C) Graph shows concentration–response curves for noradrenaline-induced muscle contraction in pulmonary artery strips from $RyR3^{+/+}$ and $RyR^{-/-}$ mice.

experiments. These data are consistent with mRNA expression in PASMCs.

Type-3 Ryanodine Receptors Mediate Hypoxia-induced, but not Noradrenaline-induced, Ca^{2+} Release and Contraction in PASMCs

Because RyR3 is expressed in PASMCs, we sought to examine if neurotransmitter-induced Ca^{2+} release was affected in PASMCs from $RyR3^{-/-}$ mice. Fig. 10 A shows an example of these experiments, in which noradrenaline (10 μM) induced similar increases in $[Ca^{2+}]_i$ in wild-type ($RyR^{+/+}$) and $RyR3^{-/-}$ mouse PASMCs. The mean increases in $[Ca^{2+}]_i$ were 358 ± 24 nM in $RyR3^{+/+}$ PASMCs (n = 8) and 331 ± 17 nM in $RyR3^{-/-}$ PASMCs (n = 9) (Fig. 10 B). Similarly, concentration–response curves for noradrenaline-induced muscle contractions were not altered in pulmonary artery strips from $RyR3^{-/-}$ mice (Fig. 10 C).

Next we determined if hypoxia-induced increases in $[Ca^{2+}]_i$ were altered in $RyR3^{-/-}$ mouse PASMCs. As ex-

amples show in Fig. 11 A, hypoxia-induced increase in $[Ca^{2+}]_i$ was significantly smaller in RyR3$^{-/-}$ than that in RyR3$^{+/+}$ PASMCs. The mean hypoxia-induced increases in $[Ca^{2+}]_i$ were decreased from 379 ± 25 nM in wild-type cells (n = 12) to 200 ± 11 nM in RyR3$^{-/-}$ cells (n = 19, $P < 0.05$) (Fig. 11 B). To test the potential role of other RyR subtypes in hypoxic response, we studied the effect of the RyR antagonists ruthenium red and tetracaine on hypoxic increase in $[Ca^{2+}]_i$ in freshly isolated PASMCs from RyR3$^{-/-}$ mice. Pretreatment with ruthenium red (50 μM) for 5 min significantly inhibited hypoxic increase in $[Ca^{2+}]_i$ in RyR3$^{-/-}$ PASMCs. The mean hypoxic increases in $[Ca^{2+}]_i$ in RyR3$^{-/-}$ cells un-pretreated (n = 30) and pretreated with ruthenium red (n = 24) were 220 ± 10 and 101 ± 11 nM, respectively ($P < 0.05$). Similarly, pretreatment with tetracaine (10 μM) for 5 min could also inhibit hypoxic response in RyR3$^{-/-}$ PASMCs (Fig. 11 C). Consistent with the reduced hypoxic increase in $[Ca^{2+}]_i$ in RyR3$^{-/-}$ PASMCs, hypoxic pulmonary vasoconstriction in RyR3$^{-/-}$ mice was significantly inhibited. As summarized in Fig. 11 D, hypoxia-induced muscle tension was 25 ± 3 mg in RyR3$^{-/-}$ pulmonary artery strips (n = 8) and 37 ± 4 mg in RyR3$^{+/+}$ pulmonary artery strips (n = 7) ($P < 0.05$). Collectively, these results indicate that RyR3 mediates hypoxia-, but not noradrenaline-induced Ca^{2+} release in pulmonary artery myocytes. Moreover, RyR1 and/or RyR2 may also play a role in hypoxic response in PASMCs.

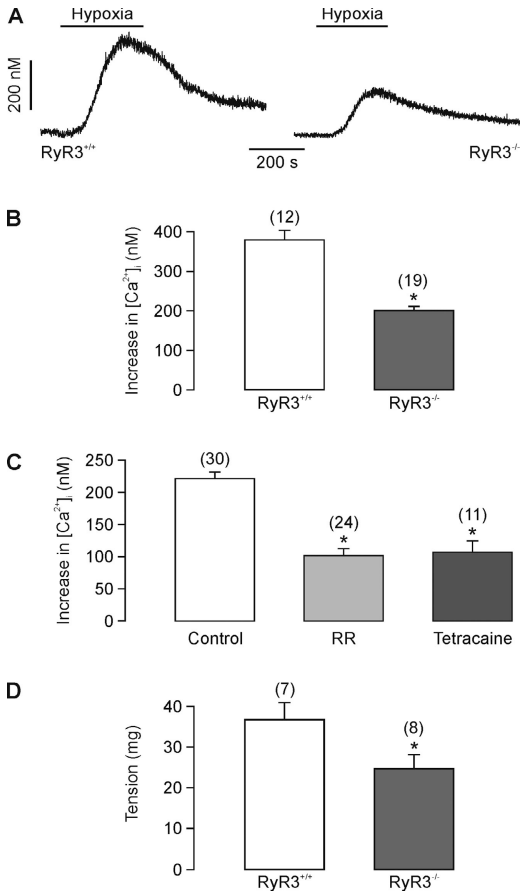

FIGURE 11. Type-3 ryanodine receptor gene knockout significantly inhibits hypoxic increase in $[Ca^{2+}]_i$ and contraction in freshly isolated mouse pulmonary artery myocytes. (A) Original recordings show hypoxic increases in $[Ca^{2+}]_i$ in a pulmonary artery myocyte from RyR3$^{+/+}$ and RyR3$^{-/-}$ mouse. (B) Summary of hypoxia-induced Ca^{2+} responses in PASMCs from RyR3$^{+/+}$ and RyR3$^{-/-}$ mice. *, $P < 0.05$ compared with RyR3$^{+/+}$. (C) Graph summarizes hypoxic increases in $[Ca^{2+}]_i$ in RyR3$^{-/-}$ mouse PASMCs pretreated without (control) and with ruthenium red (RR, 50 μM) or tetracaine (10 μM) for 5 min. *, $P < 0.05$ compared with control. (D) Summary of hypoxic vasoconstrictions in pulmonary artery strips from RyR3$^{+/+}$ and RyR3$^{-/-}$ mice. *, $P < 0.05$ compared with RyR3$^{+/+}$.

DISCUSSION

We and other investigators have recently demonstrated that prior application of caffeine to deplete SR Ca^{2+} by opening RyRs prevents subsequent neurotransmitter-induced Ca^{2+} release through IP_3Rs, and vice versa, in freshly isolated and cultured rat PASMCs (Wang et al., 2003; Zhang et al., 2003), suggesting that RyRs and IP_3Rs are functionally coupled in the SR. Consistent with this view, this study has demonstrated that dialysis of IP_3 to directly activate IP_3Rs induces Ca^{2+} release (Ca^{2+}-activated Cl^- currents) and blocks subsequent caffeine responses in freshly isolated rat PASMCs (Fig. 2 A). Conversely, prior application of caffeine to induce Ca^{2+} release abolishes subsequent IP_3-induced responses (Fig. 2 B).

It has been previously noted that caffeine inhibits IP_3-induced Ca^{2+}-activated Cl^- currents (Ca^{2+} release) in *Xenopus* oocytes, cerebellar IP_3Rs reconstituted in planar lipid bilayers, and IP_3-induced Ca^{2+} release in permeabilized A7r5 cells in the absence of ATP by affecting the binding of IP_3 to IP_3Rs (Parker and Ivorra, 1991; Bezprozvanny et al., 1994; Missiaen et al., 1994), although other investigators have shown that caffeine does not have an effect on the binding of IP_3 to its receptor (Brown et al., 1992; Toescu et al., 1992; McNulty and Taylor, 1993). To determine whether the failure of noradrenaline or IP_3 to induce Ca^{2+} release following prior application of caffeine simply reflects an inhibitory effect on IP_3Rs, we examined the effect of CMC, another RyR activator that has not been reported to inhibit IP_3Rs, on noradrenaline-induced Ca^{2+} release in freshly isolated rat PASMCs. Similar to caffeine, CMC also induces a large increase in $[Ca^{2+}]_i$ and blocks subsequent noradrenaline-induced Ca^{2+} release. As another approach to examine the specificity of caffeine as a selective agonist of RyRs in PASMCs, we performed experiments in cultured human PASMCs, since cell culture may result in significant changes in RyR expression levels and patterns in vascular SMCs, in which caffeine

is ineffective (Masuo et al., 1991; Cortes et al., 1997; Vallot et al., 2000). Consistent with these data, we have found that the RyR agonists caffeine and CMC both fail to induce Ca^{2+} release, although RyR1, RyR2, and RyR3 mRNAs are found in cultured human PASMCs. In addition, caffeine does not inhibit ATP-induced increases in $[Ca^{2+}]_i$ in these cultured cells in the presence and absence of extracellular Ca^{2+}. These findings, together with the fact that application of ATP to stimulate purinergic receptors can induce Ca^{2+} release through IP_3Rs, although also trigger Ca^{2+} influx through nonselective cation channels in a variety of cells including vascular SMCs (Tawada et al., 1987; Lagaud et al., 1996; North and Barnard, 1997; Szado et al., 2003), indicate that caffeine has no inhibitory effect on IP_3-mediated Ca^{2+} release. Taken together, our data indicate that the failure of noradrenaline and IP_3 to induce Ca^{2+} release in freshly isolated rat PASMCs in the presence of caffeine is not due to the inhibition of IP_3Rs, but rather due to prior depletion by caffeine of SR Ca^{2+} stores, where RyRs and IP_3Rs functionally overlap. In support of this view, direct measurements of SR Ca^{2+} have shown that caffeine and muscarinic receptor agonists cause identical patterns of SR Ca^{2+} depletion in gastric SMCs (White and McGeown, 2002). The reasons for the different effects of caffeine on IP_3-induced Ca^{2+} release reported by different investigators are unknown, but they may be related to different experimental conditions. For example, caffeine significantly inhibits IP_3-induced Ca^{2+} release in the absence of ATP, but not in the presence of 1.5 and 5 mM ATP (McNulty and Taylor, 1993; Missiaen et al., 1994). In addition, different cell types may show different responses to caffeine. It is known that *Xenopus* oocytes only express type-1 IP_3Rs (Parys et al., 1992), whereas vascular myocytes (e.g., PASMCs) express all three subtypes of IP_3Rs (type 1, 2, and 3 IP_3Rs) (Zheng et al., 2004). Thus, the differences in expression patterns and levels of IP_3R subtypes may also contribute to differential effects of caffeine on IP_3-induced Ca^{2+} release. This may be the case in some smooth muscle cells and species. In agreement with this view, a well-designed study using canine PASMCs has shown the functionally distinct IP_3- and ryanodine-sensitive Ca^{2+} stores (Janiak et al., 2001). Similar observation has been also observed in rabbit and guinea pig colonic SMCs (Young et al., 1999; Flynn et al., 2001).

The functional roles of RyRs have not been well established in vascular SMCs. In this study, we have found that full activation of RyRs with caffeine and IP_3Rs with noradrenaline induce equivalent Ca^{2+} release in rat PASMCs (Fig. 1), suggesting that RyRs are highly expressed. Prior application of the structurally different RyR antagonists ruthenium red, ryanodine, and tetracaine can significantly inhibit submaximal noradrenaline–induced increases in $[Ca^{2+}]_i$. Consistent with these results, these RyR antagonists shift concentration–response curves for noradrenaline-induced contraction to the right. These results suggest that Ca^{2+} released from IP_3Rs following submaximal agonist stimulation may open neighboring RyRs and then induce further Ca^{2+} release from the SR (CICR), which amplifies agonist-induced increase in $[Ca^{2+}]_i$ and contraction in PASMCs. Since it has been reported that RyR antagonists may inhibit IP_3Rs directly or indirectly (Vites and Pappano, 1992; Yamazawa et al., 1992; Iino et al., 1994; Tovey et al., 2000; Zimmermann, 2000; Flynn et al., 2001), one might argue that the inhibition of IP_3Rs could account for the effects of the RyR antagonists on noradrenaline-induced Ca^{2+} release and contraction in PASMCs. However, our data and previous reports indicate that this may not be the case in pulmonary artery (vascular) SMCS. First, none of the RyR antagonists ruthenium red, tetracaine, and dantrolene affect maximal noradrenaline–induced increase in $[Ca^{2+}]_i$ and cell contraction (Figs. 4 and 5). Second, ruthenium red, ryanodine, and tetracaine do not block ATP (10 and 100 μM)-induced increases in $[Ca^{2+}]_i$ in the presence and absence of extracellular Ca^{2+} in cultured human PASMCs that lack functional expression of RyRs (Fig. 6). Third, recent studies have shown that dialysis of RyR antibody blocks Ca^{2+} release following stimulation of α-adrenergic receptors with noradrenaline in cultured portal vein SMCs (Boittin et al., 1999), and the IP_3R antagonists xestospongin C and 2-aminoethoxydiphenyl inhibit RyR-generated Ca^{2+} sparks in portal vein myocytes (Gordienko and Bolton, 2002). Finally, photorelease of caged IP_3 can induce Ca^{2+} sparks in cultured PASMCs (Zhang et al., 2003). Taken together, the RyR antagonists may block neurotransmitter-induced Ca^{2+} release and contraction in PASMCs by specifically inhibiting RyRs, rather than by affecting IP_3Rs.

It is known that ryanodine concentrations <10 μM activate RyRs, whereas concentrations >10 μM block RyRs in isolated SR preparations (Meissner, 1986). We have found that ryanodine at 100 μM, unlike the other RyR antagonists ruthenium red, tetracaine, and dantrolene, inhibits maximal noradrenaline–induced Ca^{2+} release and associated contraction in PASMCs (Figs. 5 and 6). These results suggest that following application of ryanodine (100 μM), this agent may initially activate RyRs possibly due to the low concentration, causing partial depletion of SR Ca^{2+}.

Several studies have shown that ryanodine inhibits hypoxia-induced increases in $[Ca^{2+}]_i$ in cultured PASMCs and hypoxic pulmonary vasoconstriction in isolated pulmonary artery and lung preparations (Vadula et al., 1993; Cornfield et al., 1994; Jabr et al., 1997; Morio and McMurtry, 2002), indicating that RyRs potentially play an important role in hypoxic responses. Considering that ryanodine possibly affects the SR Ca^{2+}

(Figs. 5 and 6), we sought to examine the effects of ruthenium red and tetracaine (the RyR antagonists without affecting the SR Ca^{2+}) on hypoxic responses. As shown in Fig. 7, prior application of ruthenium red and tetracaine, similar to ryanodine, also inhibit hypoxia-induced increases in $[Ca^{2+}]_i$ in PASMCs. Consistent with these results, hypoxic pulmonary vasoconstriction is also significantly inhibited in pulmonary artery strips pretreated with ruthenium red, tetracaine, and ryanodine. Therefore, RyRs may be important targets for hypoxia, by which Ca^{2+} release from the SR contributes to hypoxic increase in $[Ca^{2+}]_i$ and contraction in PASMCs.

Several studies using RT-PCR have reported that all three RyR subtype mRNAs are expressed in aorta, cerebral, and mesenteric arteries as well as portal vein (Neylon et al., 1995; Coussin et al., 2000; Lohn et al., 2001). In contrast, other groups have shown that abundant RyR3, little RyR2, and no RyR1 mRNAs are present in aorta (Ledbetter et al., 1994; Vallot et al., 2000). Moreover, a recent study has reported that RyR1 mRNA is present in aorta with endothelium, but not in the tissue free of endothelium (Vallot et al., 2000). These conflicting data in systemic artery SMCs possibly occur due to changes in expression patterns and levels of RyR subtype mRNAs resulting from cell culture and/or due to the contamination with nonmuscle cells in experiments using vascular tissues (Vallot et al., 2000). Furthermore, there have been no reports aimed at examining mRNA expression of RyR subtypes in pulmonary artery myocytes. Therefore, we sought to examine mRNA expression of RyR subtypes in freshly isolated rat PASMCs using real-time quantitative RT-PCR. As shown in Fig. 9 B, all three RyR subtype mRNAs are expressed in freshly isolated rat PASMCs with similar expression levels. Consistent with mRNA expression, immunofluorescence staining experiments using specific anti-RyR1, anti-RyR2, and anti-RyR3 antibodies indicate that all three subtype RyR proteins are expressed in PASMCs (Fig. 9 D). In support of our findings, Zhang et al. (2003) have recently shown that RyR1 and RyR2 proteins are detected in cultured pulmonary artery myocytes by immunofluorescence staining, although a nonspecific anti-RyR2 antibody was used and RyR3 protein expression was not examined in their study.

$RyR3^{-/-}$ mice have apparently normal growth and reproduction, but show a reduction in neonatal skeletal muscle contraction, an increase in locomotor activity, as well as an impairment of hippocampal synaptic plasticity and spatial learning (Takeshima et al., 1996; Bertocchini et al., 1997; Balschun et al., 1999). A study using cerebral artery myocytes from $RyR3^{-/-}$ mice has revealed that the frequency of Ca^{2+} sparks and STOCs (spontaneous transient inward currents) are increased (Lohn et al., 2001), whereas another report has shown that caffeine- and noradrenaline-induced muscle contractions are not significantly changed in $RyR3^{-/-}$ mouse aortic arteries (Takeshima et al., 1996). In this study, we have found that submaximal noradrenaline–induced increases in $[Ca^{2+}]_i$ are similar in PASMCs from $RyR3^{-/-}$ and $RyR3^{+/+}$ mice. In parallel, concentration–response curves for noradrenaline-induced muscle contraction are unaffected in pulmonary artery strips from $RyR3^{-/-}$ mice (Fig. 10 C). In contrast, hypoxia-induced increase in $[Ca^{2+}]_i$ is significantly smaller in PASMCs from $RyR3^{-/-}$ mice than from $RyR3^{+/+}$ mice. Similarly, hypoxic pulmonary vasoconstriction is also significantly inhibited in $RyR3^{-/-}$ mice (Fig. 11). It is evident that RyR3 plays an important role in hypoxia-induced, but not neurotransmitter-induced, Ca^{2+} release and contraction in PASMCs. This fact, together with previous findings that hypoxic increase in $[Ca^{2+}]_i$ and vasoconstriction are unique cellular responses in pulmonary, but not systemic (mesenteric and cerebral), arteries (Madden et al., 1992; Vadula et al., 1993; Yuan et al., 1993; Wang et al., 2003), suggests that distinct patterns and/or levels of RyR3 expression between PASMCs and cells from the systemic circulation might account for the known differences in the response to hypoxia in these different arterial beds, although further experiments are required to confirm this view.

Our data indicate that the RyR antagonists ruthenium red and tetracaine can further, but not completely block hypoxic increase in $[Ca^{2+}]_i$ in $RyR3^{-/-}$ mouse PASMCs (Fig. 11C). This provides evidence that other RyR subtypes (RyR1 and/or RyR2) as well as additional mechanisms may also be involved in hypoxic responses in PASMCs. In reality, it is well established that hypoxia can block voltage-dependent K^+ channels (Post et al., 1992, 1995; Archer et al., 1993, 1998; Yuan et al., 1993; Wang et al., 1997a; Hulme et al., 1999), inhibit Ca^{2+}/Na^+ exchanger (Wang et al., 2000), and activate capacitative Ca^{2+} entry in PASMCs (Fantozzi et al., 2003; Lin et al., 2004; Ng et al., 2005). The blockade of voltage-dependent K^+ channels by hypoxia depolarizes cell membrane, which may presumably activate voltage-dependent Ca^{2+} channels and then cause Ca^{2+} influx across cell membrane. The hypoxic inhibition of Ca^{2+}/Na^+ exchanger can prevent intracellular Ca^{2+} removal, contributing to hypoxic increase in $[Ca^{2+}]_i$. Thus, it is apparent that multiple pathways of Ca^{2+} release, entry, and removal are likely to be responsible for hypoxic increase in $[Ca^{2+}]_i$ and associated contraction in PASMCs.

This work was supported by National Institutes of Health grants HL049426 (H.A. Singer), HL045239 (M.I. Kotlikoff), HL064043, and HL075190, and the American Heart Association (0256269T and 0340160N) (Y.-X. Wang).

Olaf S. Andersen served as editor.

Submitted: 6 December 2004
Accepted: 3 March 2005

REFERENCES

Amedee, T., W.A. Large, and Q. Wang. 1990. Characteristics of chloride currents activated by noradrenaline in rabbit ear artery cells. *J. Physiol.* 428:501–516.

Archer, S.L., J. Huang, T. Henry, D. Peterson, and E.K. Weir. 1993. A redox-based O_2 sensor in rat pulmonary vasculature. *Circ. Res.* 73:1100–1112.

Archer, S.L., J.M. Huang, H.L. Reeve, V. Hampl, S. Tolarova, E. Michelakis, and E.K. Weir. 1996. Differential distribution of electrophysiologically distinct myocytes in conduit and resistance arteries determines their response to nitric oxide and hypoxia. *Circ. Res.* 78:431–442.

Archer, S.L., E. Souil, A.T. Dinh-Xuan, B. Schremmer, J.C. Mercier, A. El Yaagoubi, L. Nguyen-Huu, H.L. Reeve, and V. Hampl. 1998. Molecular identification of the role of voltage-gated K^+ channels, Kv1.5 and Kv2.1, in hypoxic pulmonary vasoconstriction and control of resting membrane potential in rat pulmonary artery myocytes. *J. Clin. Invest.* 101:2319–2330.

Balschun, D., D.P. Wolfer, F. Bertocchini, V. Barone, A. Conti, W. Zuschratter, L. Missiaen, H.P. Lipp, J.U. Frey, and V. Sorrentino. 1999. Deletion of the ryanodine receptor type 3 (RyR3) impairs forms of synaptic plasticity and spatial learning. *EMBO J.* 18: 5264–5273.

Bertocchini, F., C.E. Ovitt, A. Conti, V. Barone, H.R. Scholer, R. Bottinelli, C. Reggiani, and V. Sorrentino. 1997. Requirement for the ryanodine receptor type 3 for efficient contraction in neonatal skeletal muscles. *EMBO J.* 16:6956–6963.

Bezprozvanny, I., S. Bezprozvannaya, and B.E. Ehrlich. 1994. Caffeine-induced inhibition of inositol(1,4,5)-trisphosphate-gated calcium channels from cerebellum. *Mol. Biol. Cell.* 5:97–103.

Boittin, F.X., N. Macrez, G. Halet, and J. Mironneau. 1999. Norepinephrine-induced Ca^{2+} waves depend on InsP(3) and ryanodine receptor activation in vascular myocytes. *Am. J. Physiol.* 277:C139–C151.

Brown, G.R., L.G. Sayers, C.J. Kirk, R.H. Michell, and F. Michelangeli. 1992. The opening of the inositol 1,4,5-trisphosphate-sensitive Ca^{2+} channel in rat cerebellum is inhibited by caffeine. *Biochem. J.* 282(Pt 2):309–312.

Collier, M.L., G. Ji, Y. Wang, and M.I. Kotlikoff. 2000. Calcium-induced calcium release in smooth muscle: loose coupling between the action potential and calcium release. *J. Gen. Physiol.* 115:653–662.

Cornfield, D.N., T. Stevens, I.F. McMurtry, S.H. Abman, and D.M. Rodman. 1994. Acute hypoxia causes membrane depolarization and calcium influx in fetal pulmonary artery smooth muscle cells. *Am. J. Physiol.* 266:L469–L475.

Cortes, S.F., V.S. Lemos, and J.C. Stoclet. 1997. Alterations in calcium stores in aortic myocytes from spontaneously hypertensive rats. *Hypertension.* 29:1322–1328.

Coussin, F., N. Macrez, J.L. Morel, and J. Mironneau. 2000. Requirement of ryanodine receptor subtypes 1 and 2 for Ca^{2+}-induced Ca^{2+} release in vascular myocytes. *J. Biol. Chem.* 275: 9596–9603.

Dipp, M., P.C. Nye, and A.M. Evans. 2001. Hypoxic release of calcium from the sarcoplasmic reticulum of pulmonary artery smooth muscle. *Am. J. Physiol. Lung Cell. Mol. Physiol.* 281:L318–L325.

Fantozzi, I., S. Zhang, O. Platoshyn, C.V. Remillard, R.T. Cowling, and J.X. Yuan. 2003. Hypoxia increases AP-1 binding activity by enhancing capacitative Ca^{2+} entry in human pulmonary artery endothelial cells. *Am. J. Physiol. Lung Cell. Mol. Physiol.* 285: L1233–L1245.

Flynn, E.R., K.N. Bradley, T.C. Muir, and J.G. McCarron. 2001. Functionally separate intracellular Ca^{2+} stores in smooth muscle. *J. Biol. Chem.* 276:36411–36418.

Ganitkevich, V.Y., and G. Isenberg. 1995. Efficacy of peak Ca^{2+} currents (ICa) as trigger of sarcoplasmic reticulum Ca^{2+} release in myocytes from the guinea-pig coronary artery. *J. Physiol.* 484:287–306.

Gordienko, D.V., and T.B. Bolton. 2002. Crosstalk between ryanodine receptors and IP(3) receptors as a factor shaping spontaneous Ca^{2+} release events in rabbit portal vein myocytes. *J. Physiol.* 542:743–762.

Hulme, J.T., E.A. Coppock, A. Felipe, J.R. Martens, and M.M. Tamkun. 1999. Oxygen sensitivity of cloned voltage-gated K^+ channels expressed in the pulmonary vasculature. *Circ. Res.* 85: 489–497.

Iino, M., H. Kasai, and T. Yamazawa. 1994. Visualization of neural control of intracellular Ca^{2+} concentration in single vascular smooth muscle cells in situ. *EMBO J.* 13:5026–5031.

Imaizumi, Y., Y. Torii, Y. Ohi, N. Nagano, K. Atsuki, H. Yamamura, K. Muraki, M. Watanabe, and T.B. Bolton. 1998. Ca^{2+} images and K^+ current during depolarization in smooth muscle cells of the guinea-pig vas deferens and urinary bladder. *J. Physiol.* 510:705–719.

Jabr, R.I., H. Toland, C.H. Gelband, X.X. Wang, and J.R. Hume. 1997. Prominent role of intracellular Ca^{2+} release in hypoxic vasoconstriction of canine pulmonary artery. *Br. J. Pharmacol.* 122: 21–30.

Janiak, R., S.M. Wilson, S. Montague, and J.R. Hume. 2001. Heterogeneity of calcium stores and elementary release events in canine pulmonary arterial smooth muscle cells. *Am. J. Physiol. Cell Physiol.* 280:C22–C33.

Kamishima, T., and J.G. McCarron. 1996. Depolarization-evoked increases in cytosolic calcium concentration in isolated smooth muscle cells of rat portal vein. *J. Physiol.* 492:61–74.

Lagaud, G.J., J.C. Stoclet, and R. Andriantsitohaina. 1996. Calcium handling and purinoceptor subtypes involved in ATP-induced contraction in rat small mesenteric arteries. *J. Physiol.* 492:689–703.

Ledbetter, M.W., J.K. Preiner, C.F. Louis, and J.R. Mickelson. 1994. Tissue distribution of ryanodine receptor isoforms and alleles determined by reverse transcription polymerase chain reaction. *J. Biol. Chem.* 269:31544–31551.

Leijten, P.A., and C. van Breemen. 1984. The effects of caffeine on the noradrenaline-sensitive calcium store in rabbit aorta. *J. Physiol.* 357:327–339.

Lin, M.J., G.P. Leung, W.M. Zhang, X.R. Yang, K.P. Yip, C.M. Tse, and J.S. Sham. 2004. Chronic hypoxia-induced upregulation of store-operated and receptor-operated Ca^{2+} channels in pulmonary arterial smooth muscle cells: a novel mechanism of hypoxic pulmonary hypertension. *Circ. Res.* 95:496–505.

Lohn, M., W. Jessner, M. Furstenau, M. Wellner, V. Sorrentino, H. Haller, F.C. Luft, and M. Gollasch. 2001. Regulation of calcium sparks and spontaneous transient outward currents by RyR3 in arterial vascular smooth muscle cells. *Circ. Res.* 89:1051–1057.

Madden, J.A., C.A. Dawson, and D.R. Harder. 1985. Hypoxia-induced activation in small isolated pulmonary arteries from the cat. *J. Appl. Physiol.* 59:113–118.

Madden, J.A., M.S. Vadula, and V.P. Kurup. 1992. Effects of hypoxia and other vasoactive agents on pulmonary and cerebral artery smooth muscle cells. *Am. J. Physiol.* 263:L384–L393.

Masuo, M., T. Toyo-oka, W.S. Shin, and T. Sugimoto. 1991. Growth-dependent alterations of intracellular Ca^{2+}-handling mechanisms of vascular smooth muscle cells. PDGF negatively regulates functional expression of voltage-dependent, IP3-mediated, and Ca^{2+}-induced Ca^{2+} release channels. *Circ. Res.* 69:1327–1339.

McNulty, T.J., and C.W. Taylor. 1993. Caffeine-stimulated Ca^{2+} release from the intracellular stores of hepatocytes is not mediated by ryanodine receptors. *Biochem. J.* 291(Pt 3):799–801.

Meissner, G. 1986. Ryanodine activation and inhibition of the Ca^{2+} release channel of sarcoplasmic reticulum. *J. Biol. Chem.* 261: 6300–6306.

Missiaen, L., J.B. Parys, H. De Smedt, B. Himpens, and R. Casteels. 1994. Inhibition of inositol trisphosphate-induced calcium release by caffeine is prevented by ATP. *Biochem. J.* 300(Pt 1):81–84.

Morio, Y., and I.F. McMurtry. 2002. Ca^{2+} release from ryanodine-sensitive store contributes to mechanism of hypoxic vasoconstriction in rat lungs. *J. Appl. Physiol.* 92:527–534.

Neylon, C.B., S.M. Richards, M.A. Larsen, A. Agrotis, and A. Bobik. 1995. Multiple types of ryanodine receptor/Ca^{2+} release channels are expressed in vascular smooth muscle. *Biochem. Biophys. Res. Commun.* 215:814–821.

Ng, L.C., S.M. Wilson, and J.R. Hume. 2005. Mobilization of sarcoplasmic reticulum stores by hypoxia leads to consequent activation of capacitative Ca^{2+} entry in isolated canine pulmonary arterial smooth muscle cells. *J. Physiol.* 563:409–419.

North, R.A., and E.A. Barnard. 1997. Nucleotide receptors. *Curr. Opin. Neurobiol.* 7:346–357.

Pacaud, P., and G. Loirand. 1995. Release of Ca^{2+} by noradrenaline and ATP from the same Ca^{2+} store sensitive to both InsP3 and Ca^{2+} in rat portal vein myocytes. *J. Physiol.* 484:549–555.

Parker, I., and I. Ivorra. 1991. Caffeine inhibits inositol trisphosphate-mediated liberation of intracellular calcium in *Xenopus* oocytes. *J. Physiol.* 433:229–240.

Parys, J.B., S.W. Sernett, S. DeLisle, P.M. Snyder, M.J. Welsh, and K.P. Campbell. 1992. Isolation, characterization, and localization of the inositol 1,4,5-trisphosphate receptor protein in *Xenopus laevis* oocytes. *J. Biol. Chem.* 267:18776–18782.

Post, J.M., C.H. Gelband, and J.R. Hume. 1995. $[Ca^{2+}]_i$ inhibition of K^+ channels in canine pulmonary artery. Novel mechanism for hypoxia-induced membrane depolarization. *Circ. Res.* 77:131–139.

Post, J.M., J.R. Hume, S.L. Archer, and E.K. Weir. 1992. Direct role for potassium channel inhibition in hypoxic pulmonary vasoconstriction. *Am. J. Physiol.* 262:C882–C890.

Salvaterra, C.G., and W.F. Goldman. 1993. Acute hypoxia increases cytosolic calcium in cultured pulmonary arterial myocytes. *Am. J. Physiol.* 264:L323–L328.

Szado, T., K.H. Kuo, K. Bernard-Helary, D. Poburko, C.H. Lee, C. Seow, U.T. Ruegg, and C. van Breemen. 2003. Agonist-induced mitochondrial Ca^{2+} transients in smooth muscle. *FASEB J.* 17:28–37.

Takeshima, H., T. Ikemoto, M. Nishi, N. Nishiyama, M. Shimuta, Y. Sugitani, J. Kuno, I. Saito, H. Saito, M. Endo, et al. 1996. Generation and characterization of mutant mice lacking ryanodine receptor type 3. *J. Biol. Chem.* 271:19649–19652.

Tawada, Y., K. Furukawa, and M. Shigekawa. 1987. ATP-induced calcium transient in cultured rat aortic smooth muscle cells. *J. Biochem. (Tokyo).* 102:1499–1509.

Thorne, G.D., and R.J. Paul. 2003. Effects of organ culture on arterial gene expression and hypoxic relaxation: role of the ryanodine receptor. *Am. J. Physiol. Cell Physiol.* 284:C999–C1005.

Toescu, E.C., S.C. O'Neill, O.H. Petersen, and D.A. Eisner. 1992. Caffeine inhibits the agonist-evoked cytosolic Ca^{2+} signal in mouse pancreatic acinar cells by blocking inositol trisphosphate production. *J. Biol. Chem.* 267:23467–23470.

Tovey, S.C., J.L. Dyer, R.E. Godfrey, S.Z. Khan, J.G. Bilmen, M. Mezna, and F. Michelangeli. 2000. Subtype identification and functional properties of inositol 1,4, 5-trisphosphate receptors in heart and aorta. *Pharmacol. Res.* 42:581–590.

Vadula, M.S., J.G. Kleinman, and J.A. Madden. 1993. Effect of hypoxia and norepinephrine on cytoplasmic free Ca^{2+} in pulmonary and cerebral arterial myocytes. *Am. J. Physiol.* 265:L591–L597.

Vallot, O., L. Combettes, P. Jourdon, J. Inamo, I. Marty, M. Claret, and A.M. Lompre. 2000. Intracellular Ca^{2+} handling in vascular smooth muscle cells is affected by proliferation. *Arterioscler. Thromb. Vasc. Biol.* 20:1225–1235.

Vites, A.M., and A.J. Pappano. 1992. Ruthenium red selectively prevents Ins(1,4,5)P3-but not caffeine-gated calcium release in avian atrium. *Am. J. Physiol.* 262:H268–H277.

Wang, J., M. Juhaszova, L.J. Rubin, and X.J. Yuan. 1997a. Hypoxia inhibits gene expression of voltage-gated K^+ channel α subunits in pulmonary artery smooth muscle cells. *J. Clin. Invest.* 100: 2347–2353.

Wang, Q., Y.X. Wang, M. Yu, and M.I. Kotlikoff. 1997b. Ca^{2+}-activated Cl^- currents are activated by metabolic inhibition in rat pulmonary artery smooth muscle cells. *Am. J. Physiol.* 273:C520–C530.

Wang, Y.X., P.K. Dhulipala, and M.I. Kotlikoff. 2000. Hypoxia inhibits the Na^+/Ca^{2+} exchanger in pulmonary artery smooth muscle cells. *FASEB J.* 14:1731–1740.

Wang, Y.X., Y.M. Zheng, I.I. Abdullaev, and M.I. Kotlikoff. 2003. Metabolic inhibition with cyanide induces intracellular calcium release in pulmonary artery myocytes and *Xenopus* oocytes. *Am. J. Physiol. Cell Physiol.* 284:C378–C388.

White, C., and G. McGeown. 2002. Imaging of changes in sarcoplasmic reticulum $[Ca^{2+}]$ using Oregon green BAPTA 5N and confocal laser scanning microscopy. *Cell Calcium.* 31:151–159.

Yamazawa, T., M. Iino, and M. Endo. 1992. Presence of functionally different compartments of the Ca^{2+} store in single intestinal smooth muscle cells. *FEBS Lett.* 301:181–184.

Young, S.H., H.S. Ennes, J.A. McRoberts, V.V. Chaban, S.K. Dea, and E.A. Mayer. 1999. Calcium waves in colonic myocytes produced by mechanical and receptor-mediated stimulation. *Am. J. Physiol.* 276:G1204–G1212.

Yuan, X.J., W.F. Goldman, M.L. Tod, L.J. Rubin, and M.P. Blaustein. 1993. Hypoxia reduces potassium currents in cultured rat pulmonary but not mesenteric arterial myocytes. *Am. J. Physiol.* 264: L116–L123.

Zhang, W.H., R. Srihari, R.N. Day, and F. Schaufele. 2001. CCAAT/enhancer-binding protein α alters histone H3 acetylation at large subnuclear domains. *J. Biol. Chem.* 276:40373–40376.

Zhang, W.M., K.P. Yip, M.J. Lin, L.A. Shimoda, W.H. Li, and J.S. Sham. 2003. ET-1 activates Ca^{2+} sparks in PASMC: local Ca^{2+} signaling between inositol trisphosphate and ryanodine receptors. *Am. J. Physiol. Lung Cell. Mol. Physiol.* 285:L680–L690.

Zheng, Y.M., Q.B. Mei, Q.S. Wang, I. Abdullaev, F.A. Lai, H.B. Xin, M.I. Kotlikoff, and Y.X. Wang. 2004. Role of FKBP12.6 in hypoxia- and norepinephrine-induced Ca^{2+} release and contraction in pulmonary artery myocytes. *Cell Calcium.* 35:345–355.

Zimmermann, B. 2000. Control of InsP3-induced Ca^{2+} oscillations in permeabilized blowfly salivary gland cells: contribution of mitochondria. *J. Physiol.* 525:707–719.